ISSN : 0974 - 7486 Volume 10 Issue 5

Materials Science

An Indian Journal

Full Paper

MSAIJ, 10(5), 2014 [192-198]

Facile direct formation of ZnO nanoparticles from a Zn(II) coordination polymer derived from 5-(3-pyridyl)-1,3,4-oxadiazole-2-thiol and benzimidazole

Maged S.Al-Fakeh, Aref A.M.Aly*, Mahmoud A.Ghandour
Department of Chemistry, Faculty of Science, Assiut University, Assiut, (EGYPT)
E-mail : aref_20002001@yahoo.com

ABSTRACT

We report on a nano coordination polymer of Zn(II) derived from 5-(3-pyridyl)-1,3,4-oxadiazole-2-thiol (POZT) and benzimidazole (BIMZ). It was prepared, characterized and used as a precursor for zinc oxide nanoparticles (ZnO NPs) by calcination. The coordination polymer was characterized by elemental analysis, IR an UV-visible spectra fluorescence technique, X-ray powder diffraction analysis (XRD), scanning electron microscopy (SEM) and transmission electron microscopy (TEM). Thermogravimetry (TG), derivative thermogravimetry (DTG) and differential thermal analysis (DTA) have been used to study the thermal decomposition steps and to calculate the thermodynamic parameters of the nano-sized metal coordination polymer. The kinetic parameters have been calculated making use of the Coats-Redfern and Horowitz-Metzger equations. The polymer and zinc oxide possess a nanoparticle size of 20 and 34 nm, respectively. The biological activity of the coordination polymer was tested against five bacterial and six fungal strains.

KEYWORDS

Coordination polymer;
ZnO Nanoparticles;
XRD;
Thermal studies.

INTRODUCTION

The coordination polymers span scientific fields such as organic and inorganic chemistry, biology, materials science, electrochemistry, and pharmacology, having many potential applications[1]. Recently, a variety of pyridyl connectors have been extensively applied in this facet[2]. It should be noted that organosulfur compounds, which play an important role in chemical or biological processes are well documented[3]. The pyridyl oxadiazoles are suitable bridging ligands for the synthesis of coordination polymers and several papers were published on using cyclized pyridyl 1,3,4-oxadiazoles for the preparation of metal complexes[4-6]. In last decades, heterocyclic benzimidazoles, their derivatives and transition metal complexes have received considerable attention in coordination chemistry, because of their well-documented biological activities. It was found that such complexes showed larger antimicrobial activities than the free ligands[7-8]. ZnO nanoparticles is a nontoxic inorganic semiconductor which could provide such potentially useful features as high mobility, excellent chemical and thermal stability, high transparency and biocompatibility[9]. ZnO is an important electronic and

photonic material because of its wide direct band gas of 3.37 eV and ZnO nanoparticles, with different morphologies, have potential wide applications in varistors[10,11]. In addition, ZnO has much simpler crystal-growth technology, resulting in a potentially low cost for ZnO based devices. It showed wide application in dye-sensitized solar cells[12-14], anti-ultraviolet-radiation cosmetics, light-emitting device, as well as cancer detecting biosensors, antimicrobial, gas sensors and degradation of organic toxins[15-17]. Because of the quantum confinement effects, ZnO nanoparticles have some unique optical properties[18]. In this paper, we synthesized and characterized a new coordination polymer derived from the bridging ligand 5-(3-pyridyl)-1,3,4-oxadiazole-2-thiol, benzimidazole and Zn(II). The resulting coordination polymer was used as a precursor for synthesis of nanoparticles of ZnO.

EXPERIMENTAL

Materials and physical measurements

The reagents and solvents employed were commercially available and used as received without further purification. Figure 1 shows the structure of the ligands.

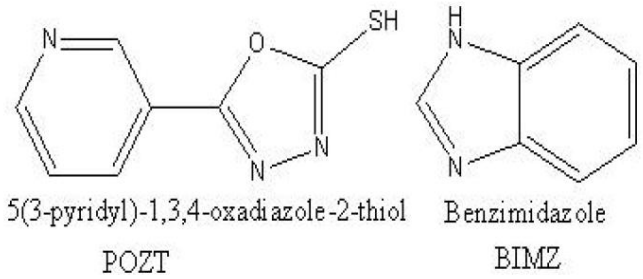

Figure 1 : Chemical structure of POZT and BIMZ

The C.H.N.S (carbon, hydrogen, nitrogen and sulphur) were performed using Analyischer Funktionstest Vario El Fab-Nr.11982027 elemental analyzer. Infrared spectrum was recorded as KBr disks (400-4000 cm^{-1}) with a FT-IR spectrophotometer model Thermo-Nicolet-6700 FTIR and the electronic spectrum was obtained using a Shimadzu UV-2101 PC spectrophotometer. The conductance was measured using a conductivity Meter model 4310 JENWAY. Thermal studies were carried out in dynamic air on a Shimadzu DTG 60-H thermal analyzer at a heating rate 10 °C min^{-1}. XRD patterns were obtained an model PW 1710 control unit Philips, anode material Cu 40 K.V 30 M.A optics: automatic divergence slit. Scanning electron microscope was of the type JEOL JFC-1100 E ION SPUTTERING DEVICE, JEOL JSM-5400 LV SEM. SEM specimen was coated with gold to increase the conductivity. Transmission electron microscope of the type JEOL JEM-100 CX II ELECTRON MICROSCOPE was used. For the biological activity, all microbial strains were kindly provided by the Assiut University Mycological Centre (AUMC), Egypt. These strains are common contaminants of the environment in Egypt and some of which are involved in human and animal diseases (Candida albicans, Geotrichum candidum, Scopulariopsis brevicaulis, Aspergillus flavus, Staphylococcus aureus), plant diseases (Fusarium oxysporum) or frequently reported from contaminated soil, water and food substances (Escherichia coli, Bacillus cereus, Pseudomonas aeruginosa and Serratia marcescens). To prepare inocula for bioassay, bacterial strains were individually cultured for 48 h in 100 ml conical flasks containing 30 ml nutrient broth medium. Fungi were grown for 7 days in 100 ml conicals containing 30 ml Sabouraud's dextrose broth. Bioassay was done in 10 cm sterile plastic Petri plates in which microbial suspension (1 ml/plate) and 15 ml appropriate agar medium (15 ml/plate) were poured. Nutrient agar and Sabouraud's dextrose agar were respectively used for bacteria and fungi. After solidification of the media, 5 mm diameter cavities were cut in the solidified agar (4 cavities/plate) using sterile cork borer. The chemical compounds dissolved in dimethyl sulfuxide (DMSO) at 2%w/v (=20 mg/ml) were pipetted in the cavities (20 ul /cavity). Cultures were then incubated at 28°C for 48 h in case of bacteria and up to 7 days in case of fungi. Results were read as the diameter (in mm) of inhibition zone around cavities[19]

Synthesis of $\{[Zn(POZT)(BIMZ)(ace)(H_2O)].H_2O\}_n$

POZT (0.1 g, 0.5 mmol) dissolved in 15 ml methanolic solution was added to 15 ml of $Zn(CH_3COO)_2.2H_2O$ (0.12 g, 0.5 mmol). The solution mixture was then stirred for about 10 min and an methanolic solution of BIMZ (0.06g, 0.5 mmol) was then added. The solution mixture was heated on a water bath for about 40 min whereupon a white precipitate was separated which was filtered off, washed with

Full Paper

ethanol and dried over $CaCl_2$. Anal. Calc. for $C_{16}H_{16}N_5O_5SZn$: C, 42.15; H, 3.54; N, 15.36; S, 7.03. Found: C, 42.95; H, 4.40; N, 15.95; S, 6.17. IR data: νOH 3498 (w), 3200 (m), νC=N 1610 (s), νC-N 1472 (s), 902 (m), νM-O 542 (m), νM-N 436 (m) cm^{-1}, m.p. 260 °C.

Formation of ZnO nanoparticles

By calcining the prepared coordination polymer in air at 500 °C with a calcination time of 3 hours afforded ZnO nanoparticles.

RESULTS AND DISCUSSION

The reaction of zinc(II) with 5-(3-pyridyl)-1,3,4-oxadiazole-2-thiol and benzimidazole proceeds readily according to equation to form the mixed ligand coordination polymer. This compound is stable in air and insoluble in common organic solvents but partially soluble in DMSO. The conductivity was measured in DMSO using 10^{-3} M solutions of the complex. The conductance value indicates the non-electrolyte nature of the coordination polymer.

$$Zn(ace)_2.2H_2O + POZT + BIMZ \xrightarrow[NaOH]{EtOH} \{[Zn(POZT)(BIMZ)(ace)(H_2O)].H_2O\}_n + CH_3COOH$$

The main IR bands of the prepared compound are cited in the experimental part. The band observed at 1610 cm^{-1} region is assigned to the υ(C=N) stretching vibration of the POZT[20]. BIMZ exhibits two bands at 902 and 1472 cm^{-1} which can be attributed to υ(C-N) ring vibrations[21]. Furthermore, the band at 3498 cm^{-1} in the spectrum of the complex can be correlated with νOH of water of crystallization[22] whereas the band at 3200 cm^{-1} is ascribed to the coordinated water molecule[23]. The complex shows two bands due to ν_{as}(COO) and ν_s(COO) of the acetate moiety at 1562 and 1437 cm^{-1}, respectively. This defines a bidentate chelating acetate group ("$\nu = \nu_{as} - \nu_s = 125\ cm^{-1}$)[24,25]. Metal-oxygen and metal-nitrogen bonding is manifested by the appearance of two bands at 542 cm^{-1} and 436 cm^{-1}, respectively[26] (Figure 2).

Electronic spectra

The electronic spectra of the mixed ligand complex and zinc oxide nanoparticle are recorded in dimethylsulphoxide (DMSO). The spectrum of the complex displays two distinct bands at 35,714 and 27,173 cm^{-1} which are attributed to π'!π* and n'!π* transitions within the POZT and BIMZ moieties, respectively[20,21]. The structure of the zinc coordination polymer can be postulated as follows:

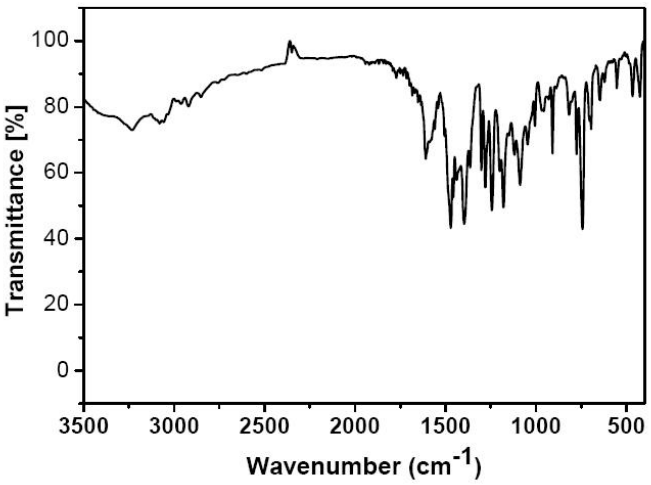

Figure 2 : FT-IR of Zn(II) coordination polymers

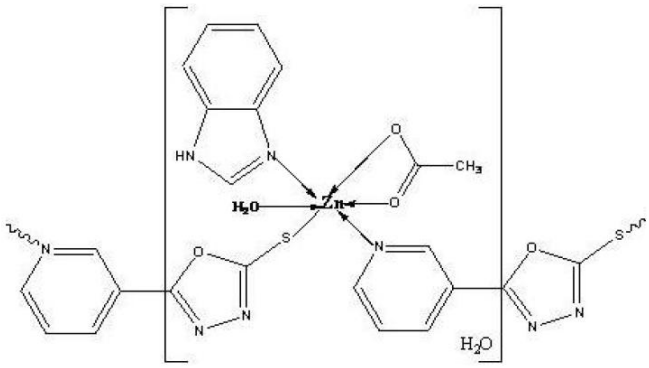

Figure 3 : Structure of $\{[Zn(POZT)(BIMZ)(ace)(H_2O)].H_2O\}_n$

Figure 4. shows the UV-vis absorption spectra of ZnO nanoparticles. It is apparent that the spectra exhibit a band absorpition edge at 348 nm[27].

Figure 5. Shows the excitation and emission spectra of ZnO NPs. The spectrum obtained under 330 nm excitation exhibits an emission at ~ 455 nm.

Thermal analysis

In dynamic air the thermal decomposition of the complex has been investigated from ambient temperature to 750 °C. The thermogram of this compound shows five decomposition steps (Figure6), namely at 30-86, 87-180, 181-266, 267-480 and 481-750 °C. The first and second stages correspond to the detach-

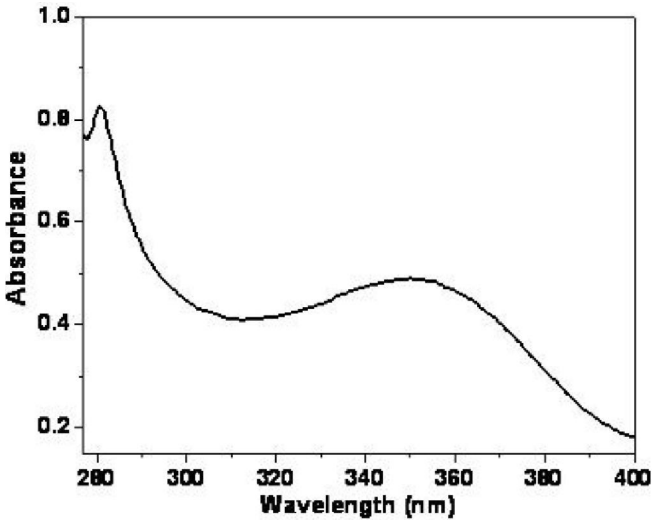

Figure 4 : UV-vis absorption spectra of the ZnO nanoparticles.

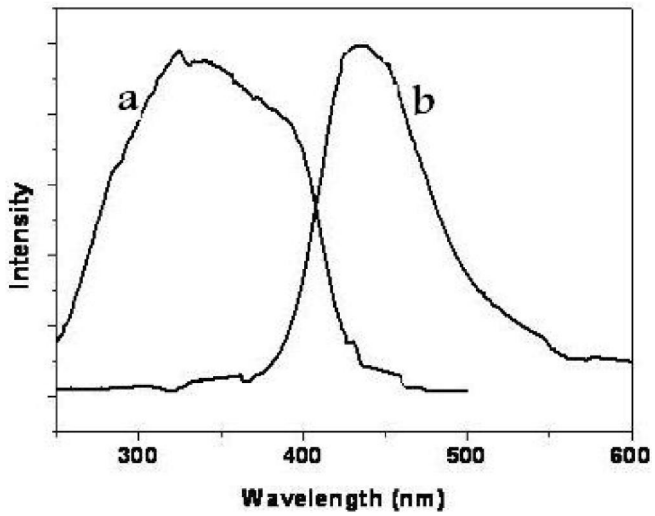

Figure 5 : Fluorescence spectra of ZnO nanoparticles a) excitation and b) emission at room temperature (λ_{ex} = 330).

ment of the coordinated and the crystalline water molecules (calc. 7.90 %, found 7.70 %). The DTG curve displays this step at two minima at 54 and 105 °C and two endothermic peaks at 56 and 107 °C in the DTA trace. The third step represents a mass loss indicating the release of an acetic acid molecule (calc. 12.95 %, found 11.27 %) (DTG peaks at 238 °C) with a broad exothermic peak in the DTA trace at 239 °C. The forth and fifth stages correspond decomposition of the rest of the organic ligands (calc. 65.22 %, found 64.24 %) (DTG peaks at 298 and 533 °C) with two exothermic peak in the DTA trace at 300 and 535 °C. The final product was identified on the basis of mass loss consideration as zinc oxide (calc. 17.85 %, found 16.79 %) as illustrated in Scheme (1)

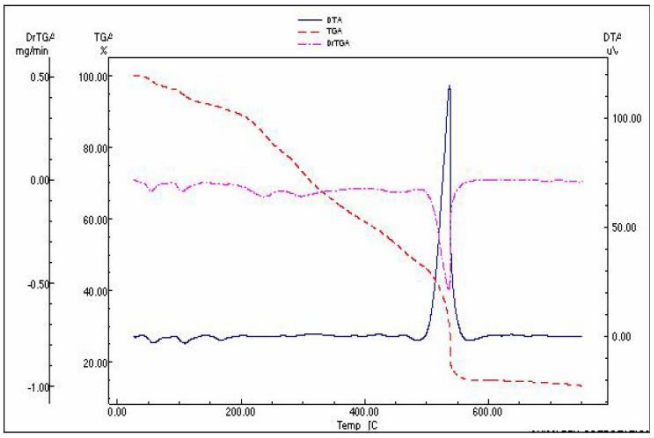

Figure 6 : TG, DTG and DTA thermograms of the Zn(II) compound in dynamic air.

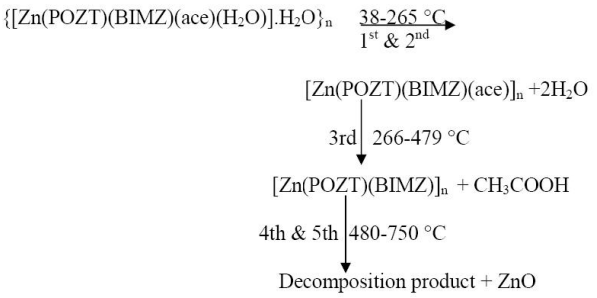

Scheme (1).

Kinetic analysis

Non-isothermal kinetic analysis of the coordination polymer was carried out applying two different procedures: the Coats-Redfern[28] and the Horowitz-Metzger[29] methods. The kinetic and thermodynamic parameters for the zinc(II) compound is calculated for the 5th step according to the above two methods and are cited in TABLE 2. This step represents a non overlapping step with a sharp DTG and DTA maxima.

TABLE 1 : Thermal decomposition data of the zinc(II) compound in dynamic air.

Step	TG/DTG			MassLoss(%)
	Ti	Tm	Tf	
1st	30	54	86	3.58
2nd	87	105	180	4.12
3rd	181	238	266	11.27
4th	267	298	480	30.14
5th	481	535	750	34.10

Ti=Initial temperature, Tm=Maximum temperature, Tf=Final temperature.

Full Paper

TABLE 2 : Kinetic and thermodynamic parameters for the thermal decomposition of the Zn(II) compound.

Step	Coats-Redfern equation				ΔS*	ΔH*	ΔG*
	r	n	E	Z			
5th	0.9999	2.00	322.3	6.44 x 10^3	-180.4	315.5	464.3

E in kJ mol^{-1} , "H*, "G* are in kJ mol^{-1} and "S* in kJ mol^{-1} K^{-1}

Negative "S* value for the decomposition of the Zn(II) compound suggest that the activated complex is more ordered than the reactants and that the reactions are slower than normal[30]. The positive value of "G* indicate that the decomposition reaction is not spontaneous.

X-ray powder diffraction of the coordination polymer and zinc oxide nanoparticles

The X-ray powder diffraction patterns were recorded for the coordination polymer Zn(II) and ZnO nanoparticles. The diffraction patterns indicate that the compounds are crystalline. The crystal lattice parameters were computed with the aid of the computer program TREOR. The crystal data for Zn(II) and mixed-ligand compound belong to the crystal system triclinic whereas the ZnO nanoparticles was belong to the hexagonal system. The significant broadening of the diffraction patterns suggests that the particles are of nanometer dimensions. XRD of compound ZnO nanoparticles is depicted in Figure 7, Scherrer's equation was applied to estimate the particle size of the compounds:

$$D = K\lambda / \beta\cos\theta$$

where K is the shape factor, λ is the X-ray wavelength typically 1.54 Å, β is the line broadening at half the maximum intensity in radians and θ is Bragg angle, D is the mean size of the ordered (crystalline) domains, which may be smaller or equal to the grain size. The crystal data together with the particle size are recorded in TABLE 3.

TABLE 3 : X-ray diffraction crystal data of the Zn(II) compound and ZnO.

Parameters	Zn(II) compound	ZnO
Empirical formula	$C_{16}H_{16}ZnN_5SO_5$	ZnO
Formula weight	455.83	81.39
Crystal system	triclinic	hexagonal
a (Å)	4.483	3.253
b (Å)	9.590	3.253
c (Å)	10.978	5.211
α (°)	73.959	90.00
β(°)	86.250	90.00
γ(°)	104.182	120.00
Volume of unit cell(Å3)	435.34	47.74
Particle size(nm)	20	34

Electron microscopy (SEM and TEM)

The scanning electron and transmission micrographs of zinc oxide nanoparticles are given in (Figures 8-9). In order to elucidate the ZnO nanoparticles morphologies, scanning electron microscopy (SEM) was performed which demonstrates clearly the formation of ZnO nanoparticles. It can be clearly seen that the nanoparticles have a Bacillary-like or series shape. Fig-

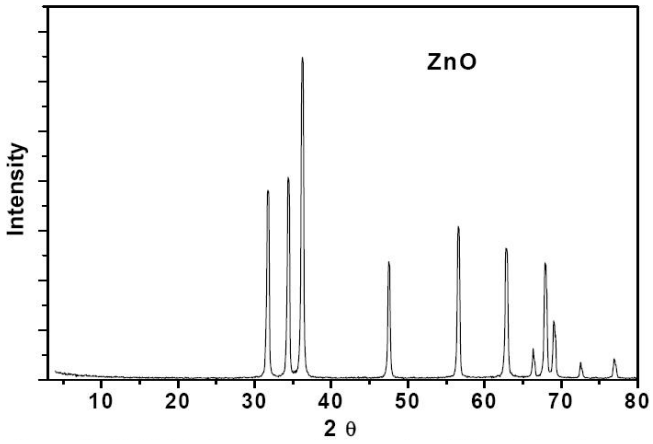

Figure 7 : XRD ZnO nanoparticles produced by calcination of {[Zn(POTZ)(BIMZ)(ace)(H_2O)].H_2O}$_n$

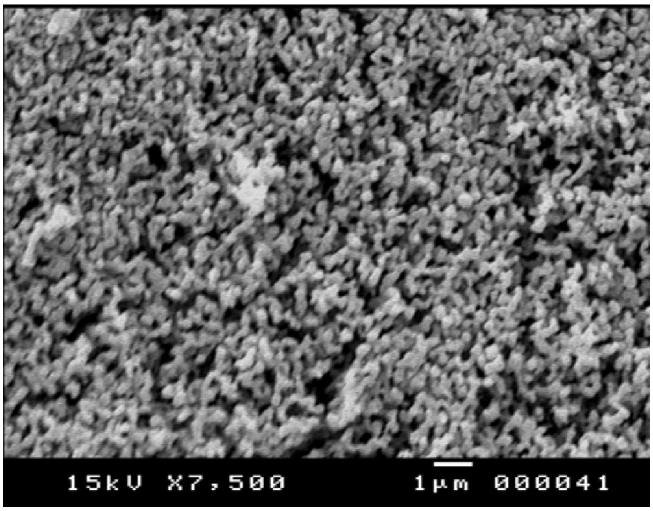

Figure 8 : SEM of ZnO nanoparticles.

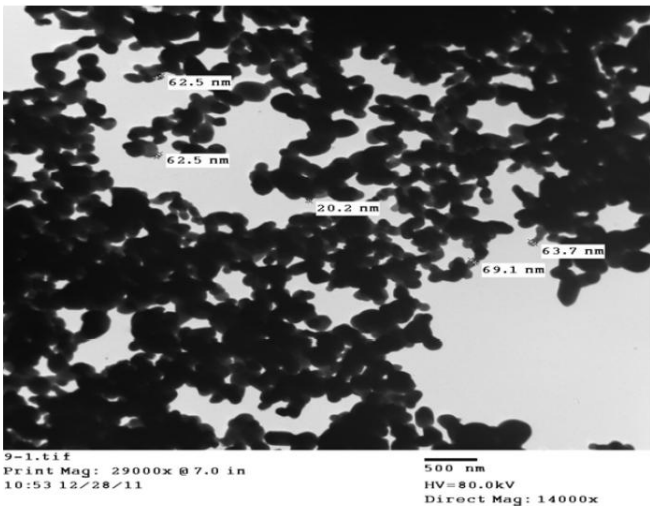

Figure 9 : TEM of ZnO nanoparticles.

ure 8. shows the transmission electron microscopy (TEM) image of ZnO nanoparticles. This image shows that the size of ZnO NPs is very consistent.

Antimicrobial activity

The antimicrobial activity of the Zn(II) coordination polymer was investigated against five bacterial and six fungal strains. In testing the antibacterial and antifungal activity of the compound we used more than one test organism to increase the chance of detecting the antibiotic principles in the tested materials. The data showed that in some cases the coordination polymer has a similar antimicrobial and antifungal activity than the selected standards (chloramphenicol and clotrimazole) (TABLE 4). Figures (10&11) show the antimicrobial effect for the compound.

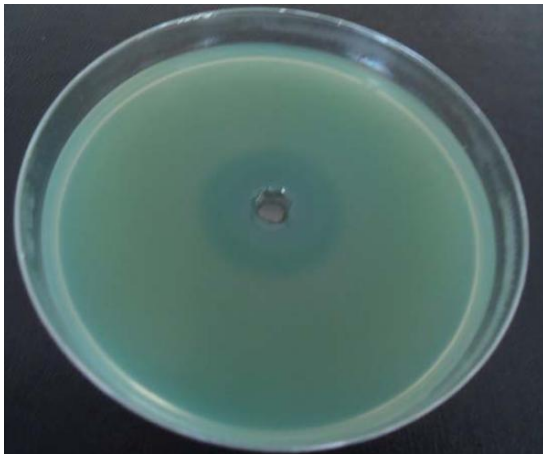

Figure 10 : Microbiological screening of the zinc compound against Pseudomonas aeruginosa (-ve).

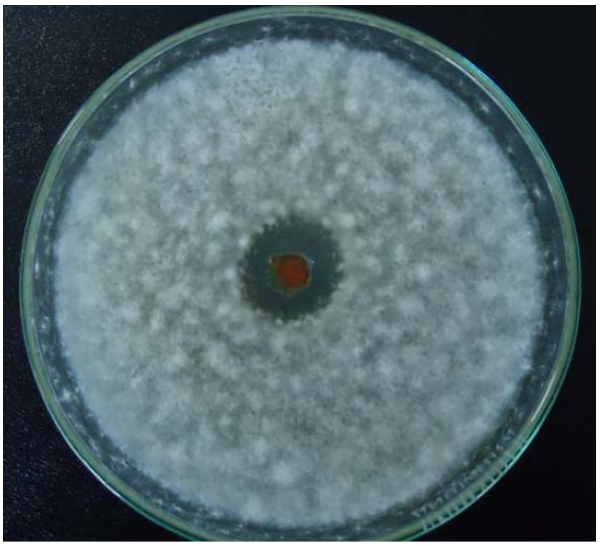

Figure 11 : Microbiological screening of the zinc compound against Geotrichum candidum.

TABLE 4 : Microbiological screening of the Zn(II) compound.

B. Cereus (G+ve)	S. aureus (G+ve)	S. Marcescens (G-ve)	E. coli (G-ve)	P. aeruginosa (G-ve)	T. rubrum	A. flavus	C. albicans	F. oxysporm	G. candidum	S. brevicaulis
11	12	0	14	14	0	0	8	0	12	14

CONCLUSION

In conclusion, the spherical shaped aggregates of ZnO nanoparticles were synthesized by calcination method. Results of x-ray pattern show that all peaks can be well indexed to the phase of ZnO. SEM and TEM micrographs show that there are many micropores among the nanocrystals for the samples calcined at 500 ºC for 3 h. The crystal size is less than 100 nm. This results show that the particle size of the ZnO is about 34 nm.

REFERENCES

[1] Fromm K.Coord; Chem.Rev., **252**, 856 **(2008)**.
[2] Z.H.Zhang, Y.L.Tian, Y.M.Guo; Inorg.Chim.Acta, **360**, 2783 **(2007)**.

[3] S Oae; Structure and Mechanism. CRC Press Boca Raton FL, **(1992)**.

[4] Z.H.Zhang, C.P.Li, G.M.Tang, Y.L.Tian, Y.M.Guo; Inorg.Chem.Com., **11**, 326 **(2008)**.

[5] YT Wang, GM.Tang; Inorg.Chem.Commun, **10**, 53 **(2007)**.

[6] Y.T.Wang, G.M.Tang, Z.W.Qiang; Polyhedron, **26**, 4542 **(2007)**.

[7] F.Gumus, O.Algul,G.Eren, H.Eroglu, N.Diril, S.Gur, A.Ozkul ; Eur.J.Med.Chem.,**38**, 473 **(2003)**.

[8] D.Kumar Sau, R.J.Butcher, S.Chaudhuri, N.Saha ; Molec.Cell.Biochem., **253**, 21 **(2003)**.

[9] L.Schmidt-Mende, J.L.MacManus-Driscoll ; Mater.Today, **10**, 40 **(2007)**.

[10] D.R.Clarke; Journal of the American Ceramic Society, **82**, 485 **(1999)**.

[11] N.T.Hung, N.D.Quang, S.Bernik; J. of Materials Research, **16**, 2817 **(2001)**.

[12] K.Funabiki, N.Sugiyama, H.Iida, J.-Ye Jin, T.Yoshida, Y.Kato, H.Minoura, M.Matsui; J.Fluorine Chem., **127**, 257 **(2006)**.

[13] M.Quintana, T.Edvinsson, A.Hagfeldt, G.Boschloo; J.Phys.Chem., **C111**, 1035 **(2007)**.

[14] X.Sheng, Y.Zhao, J.Zhai, L.Jiang, D.Zhu; Appl.Phys., **A87**, 715 **(2007)**.

[15] S.Krishnamoorthy, A.Iliadis, T.Bei, P.G.Chrousos; Biosens.Bioelectron., **24**, 313 **(2008)**.

[16] A.Otsuka, K.Funbiki, N.Sugiyama, T.Yoshida, H.Minoura, M.Matsui; Chem.Lett., **35**, 666 **(2006)**.

[17] Y.-L.Wang, H.S.Kim, D.P.Norton, S.J.Pearton, F.Ren; Appl.Phys.Lett., **92**, 112101 **(2008)**.

[18] U.Koch, A.Fojtik, H.Weller, A.Henglein; Chem.Phys.Lett., **122**, 507 **(1985)**.

[19] K.J.Kwon-Chung, J.E.Bennett; Medical mycology, Lea & Febiger, Philadelphia, **(1992)**.

[20] M.Singh, R.J.Butcher, N.K.Singh; Polyhedron, **27**, 3151 **(2008)**.

[21] K.S.Banu, S.Mondal, A.Guha, S.Das; Polyhedron, **30**, 163 **(2011)**.

[22] A.Bravo, J.Anacona; Transition.Met.Chem., **26**, 20 **(2001)**.

[23] T.Rakha; Synth.React.Inorg.Met.- Org.Chem., **30**, 205 **(2000)**.

[24] K.Nakamoto; Infrared and Raman Spectra of Inorganic and Coordination Compounds, 4th Edition, John Wiely and Sons, New York, **(1986)**.

[25] G.B.Deacon, R.J.Phillips; Coord.Chem.Rev., **33**, 227 **(1980)**.

[26] M.C.Jain, R.K.Sharma, P.C.Jain; Gazz.Chim.Ital., **109**, 601 **(1979)**.

[27] M.El-kemary, H.El-Shamy, I.El-Mehasseb, J. of Luminescence, **130**, 2327 **(2010)**.

[28] A.Coats; J.Redfern, Nature., **20**, 68 **(1964)**.

[29] H.Horowitz, G.Metzger; Anal.Chem., **35**, 1464 **(1963)**.

[30] J.Hill, R.J.Magee; Reviews Inorg.Chem., **3**, 141 **(1981)**.